Research paper

Multiple states in the flow through a sluice gate

D. P. VIERO, PhD, Researcher, *Department of Civil, Environmental and Architectural Engineering, University of Padova, Italy*
Email: daniele.viero@unipd.it (author for correspondence)

A. DEFINA, PhD, Full Professor, *Department of Civil, Environmental and Architectural Engineering, University of Padova, Italy*
Email: andrea.defina@unipd.it

ABSTRACT

This paper addresses the problem of hydraulic hysteresis for a supercritical open channel flow approaching a sluice gate when subcritical flow can establish downstream, against the gate. The possible flow configurations across the gate are classified on the basis of the Froude number of the incoming and downstream flows, and of the ratio of gate opening to the upstream supercritical flow depth. Within the above parameter space, two regions exist in which the problem admits a dual solution, that is, two different flow configurations can establish for the same gate opening and undisturbed flow conditions. In one of these regions, both smooth flow (i.e. the fluid flows under the gate without interacting with the gate) and free outflow conditions can establish; in the other region, both smooth flow and submerged flow can establish. For flow conditions in the above regions, the configuration that actually establishes depends on the previous history of the flow, thus implying the hysteretic character of the flow.

Keywords: Control structures, Flow-structure interactions, Hydraulic hysteresis, Multiple states, Open-channel flow

1   Introduction

When a supercritical open channel flow approaches an obstruction, flow and geometry conditions can be such that two different flow configurations can establish across the obstruction. This behaviour is said to be hysteretic since the configuration that actually establishes depends on the past history of the flow (Defina and Susin, 2003, 2006).

Hydraulic hysteresis has been widely studied both theoretically and experimentally. The hysteretic behaviour of flow approaching a sill in a channel of constant width was studied extensively (Abecasis and Quintela, 1964; Austria, 1987; Baines, 1984; Baines and Whitehead, 2003; Lawrence, 1987; Mehrotra, 1974; Muskatirovic and Batinic, 1977; Pratt, 1983; Sadeghfam, Khatibi, Hassanzadeh, Daneshfaraz, & Ghorbani, 2017). The occurrence of hydraulic hysteresis in the case of a channel contraction was demonstrated by Akers and Bokhove (2008), Defina and Viero (2010), and by Sadeghfam et al. (2017).

Hysteresis that can develop in a supercritical channel flow approaching a sluice gate was assessed by Defina and Susin (2003), who proposed a simple theory to predict its occurrence and to classify possible flow regimes in the vicinity of the gate. They also verified the theory by performing an in-depth experimental study, and showed that both undisturbed and free outflow conditions may exist for the same gate opening within a wide range of flow parameters.

However, all the above studies assume supercritical flow conditions close downstream of the obstacle. In that case, the hysteretic behaviour is controlled by the obstacle characteristics and the

upstream flow conditions; the two flow configurations that can occur are (i) the supercritical flow remains supercritical through the obstacle, or (ii) a supercritical to subcritical transition (i.e. a hydraulic jump) occurs upstream of the obstacle, and critical condition establishes at the obstacle.

Recently, Viero & Defina (2017) demonstrated that hydraulic hysteresis can occur also when subcritical flow can establish just downstream of, and possibly against an obstacle. In the presence of a downstream subcritical flow against the obstacle, the problem complicates since it has one more degree of freedom (i.e. the downstream flow conditions), and the number of possible flow configurations increases significantly. The two flow configurations that can establish through the obstacle are (i) supercritical smooth flow configuration, i.e. the flow remains supercritical in passing the obstacle and supercritical to subcritical transition occurs downstream of the obstacle; (ii) subcritical smooth flow configuration, i.e. the supercritical to subcritical transition occurs upstream of the obstacle and the flow remains subcritical through (and downstream of) the obstacle. For illustration purposes, Viero & Defina (2017) applied the theory to two specific obstacles, namely a raised bed hump and a channel contraction.

By extending the work of Defina and Susin (2003) in the light of the more general framework of Viero & Defina (2017), i.e. the possible presence of a downstream subcritical flow, the present work focuses on the flow through a vertical sluice gate, for which the hysteretic behaviour concerns the possibility that, for a given gate opening, a supercritical approaching flow may either remain supercritical without interacting with the gate, or undergo a supercritical to subcritical transition upstream of the gate, with the flow through the gate that can be either free or submerged depending on the downstream flow conditions. Anyway, the state that actually establishes is determined by the past history of the flow.

The sluice gate is a relatively simple device that can lead to an extremely involved hydraulic behaviour, and for this reason it is worth studying. Practical applications related to this study can also be found: for example, to divert water from relatively steep channels with large bedload, the use of gates rather than weir sills to control the upstream level, and hence the diverted discharge, is often preferred; in addition, for the major flowrates, the possible presence of downstream obstacle (bridges, channel contractions, etc.) can force subcritical flow downstream the gate.

The paper is outlined as follows. First, the domains of existence are derived theoretically for all the different flow configurations that can establish through the gate, approached by a supercritical flow and in the presence of a downstream subcritical flow. Conditions for the existence of a dual solution, when two different flow configurations can establish for the same gate opening and undisturbed flow conditions, are then identified. A brief discussion closes the paper.

2   Single and double states

In order to find if, and possibly when, a dual solution exists in the flow through a sluice gate when subcritical flow is allowed to establish downstream against the gate, and in order to make the analysis as clear as possible, the following steps are taken: (i) the domains of existence of all the different flow configurations that can establish through the gate are identified separately; (ii) by superimposing these domains of existence, the dual solution domains, in which two different flow configurations can establish for the same gate opening and undisturbed flow conditions, are identified as the regions where the domains of existence overlap.

The solution, i.e. the domain of existence of the different flow configurations across the gate, can be represented in the 3D space of parameters $(a/Y_u, \mathsf{F}_u, \mathsf{F}_d)$, where a is the gate opening, Y_u is the depth of the incoming flow, which is assumed as the vertical length scale (Viero, Peruzzo, & Defina, 2017), $\mathsf{F} = U/gY$ is the Froude number, U is the bulk flow velocity, g is gravity, and the subscripts "u" and "d" denote the cross sections just upstream and downstream of the gate, respectively. For clarity, the domains of existence of the different flow configurations are represented in the plane $(\mathsf{F}_u, a/Y_u)$, for given values of the downstream Froude number, F_d.
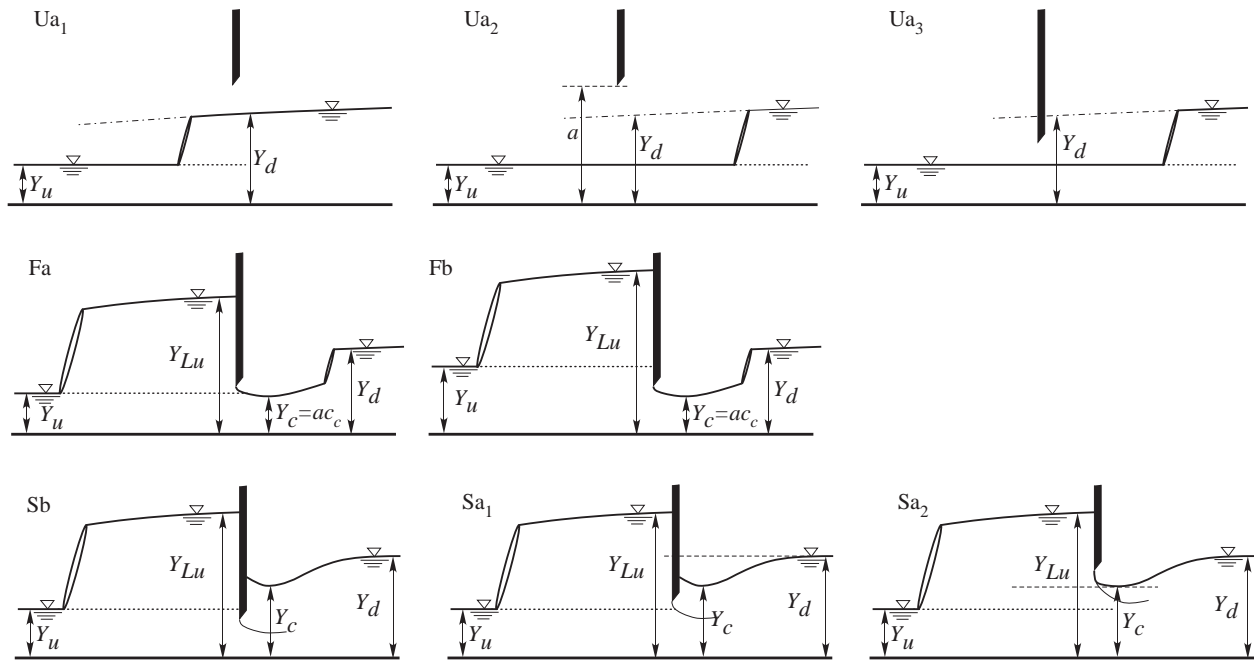
Figure 1   Steady flow through a sluice gate, with notation. Dotted lines denotes upstream undisturbed flow (if unaffected by the downstream subcritical flow or by the gate), dash-dotted lines denote the undisturbed downstream flow profile (if unaffected by the upstream supercritical flow or by the gate).

In the theoretical analysis, the flow is assumed one-dimensional and the pressure, away from the gate, is assumed hydrostatic. In applying energy and momentum balance equations across and just downstream the gate, friction and bed slope are neglected.

A dual solution can exist only if the incoming flow is supercritical (e.g. Defina and Susin, 2006); hence, hereinafter, we assume that the upstream flow has a Froude number greater than one. In this case, the different flow states that can establish through a vertical sluice gate are shown in Fig. 1. The labels used to distinguish the different flow configurations are so constructed; the first character distinguishes the case when the flow does not interact with the gate (U) from free (F) or submerged (S) outflow; the second character indicates that the depth of the incoming supercritical flow is smaller (a) or greater (b) than the gate opening; the third character (subscripts 1, 2, or 3) distinguishes among the possible configurations belonging to the same class, which is identified by the first two characters.

Among the configurations of Fig. 1, those with the upstream flow depth smaller than the gate opening are the most interesting, since only in this case two different stable configurations can occur for the same gate opening and flow conditions. Also interesting is the Sa_2 configuration in which the flow depth at the *vena contracta*, Y_c, controlled by downstream flow, turns out to be smaller than the gate opening; this submerged flow condition is sometimes referred to as partially submerged flow (Belaud, Cassan, & Baume, 2009).

The theoretical findings by Defina and Susin (2003), which only refer to the case when supercritical flow conditions occur downstream of the gate, are preliminarily re-derived following the approach used in the present work. These results are of interest since they represents the extreme case in which the downstream subcritical flow does not affect the flow through the gate. This condition occurs when $F_d \geq 1$ or when F_u is large enough such that either the incoming supercritical flow flowing below the gate, or the jet of fluid issuing from under the gate in the case of free outflow, have large enough momentum to push the subcritical flow far downstream from the gate. In addition, here we scale the gate opening by the flow depth of the supercritical incoming flow rather than by the critical depth.

3

In general, a dual solution exists, i.e. two different flow states can establish, only if the incoming supercritical flow can flow under the gate without interacting with it. Trivially, this necessary condition reads

$$\frac{a}{Y_u} \geq 1 \tag{1}$$

The lower boundary of the hysteresis region in the ($\mathsf{F_u}$, a/Y_u) plane is then given by the endpoint of the above interval, i.e. $a/Y_u=1$.

One of the two possible flow states is when the incoming flow does not actually interact with the gate. This flow configuration is referred to as supercritical smooth flow configuration (see, for example, flow configurations $\mathrm{Ua_2}$ and $\mathrm{Ua_3}$ in Fig. 1). The other flow state that can establish through the gate is the free outflow configuration (see, for example, configurations Fa or Fb in Fig. 1). In order for this configuration to be stable, the momentum of the incoming flow must be smaller than or equal to the momentum of the subcritical flow establishing just upstream of the gate, i.e.:

$$Y_u^{conj} \leq Y_{Lu} \tag{2}$$

where Y_u^{conj} is the conjugate water depth (or sequent depth) of the incoming supercritical flow, and Y_{Lu} is the subcritical depth that establishes just upstream of the gate (Fig. 1). The upper boundary of the hysteresis region is then given by the endpoint of the above interval (i.e. $Y_u^{conj} = Y_{Lu}$), which is rewritten as

$$Y_u \frac{R_u}{2} = Y_{Lu} \tag{3}$$

with

$$R_u = -1 + \sqrt{1 + 8\mathsf{F_u^2}} \tag{4}$$

The flow depth Y_{Lu} is related to the flow depth at the *vena contracta*, ac_c, through the energy balance equation

$$Y_{Lu} + \frac{q^2}{2gY_{Lu}^2} = ac_c + \frac{q^2}{2g(ac_c)^2} \tag{5}$$

where q is the flow rate per unit width, a is the gate opening, and c_c is the contraction coefficient, which is a function of the relative gate opening a/Y_{Lu}.

Equation (5) can be rewritten as

$$\frac{Y_{Lu}}{ac_c} = 1 + \frac{\mathsf{F_c^2}}{2}\left[1 - \left(\frac{Y_{Lu}}{ac_c}\right)^{-2}\right] \tag{6}$$

with $\mathsf{F_c}$ the Froude number at the *vena contracta*.

Equation (6) has three solutions; one is $Y_{Lu} = ac_c$ which is physically unacceptable; among the other two solutions, one is discarded because it provides a negative value for Y_{Lu}, the other reads

$$\frac{Y_{Lu}}{ac_c} = \frac{\mathsf{F}_c^2}{4}\left(1 + \sqrt{1 + \frac{8}{\mathsf{F}_c^2}}\right) \tag{7}$$

Equation (3), with Eq. (7), is rewritten as

$$\frac{R_u}{\mathsf{F}_u^{2/3}} = \frac{\mathsf{F}_c^{4/3}}{2}\left(1 + \sqrt{1 + \frac{8}{\mathsf{F}_c^2}}\right) \tag{8}$$

Recalling that the continuity equation gives $Y_x\mathsf{F}_x^{2/3} = \text{const.}$, where the subscript x denotes any generic cross section, we can write

$$\frac{a}{Y_u} = \frac{1}{c_c}\left(\frac{\mathsf{F}_u}{\mathsf{F}_c}\right)^{2/3} \tag{9}$$

From a practical standpoint, for each $\mathsf{F}_u \geq 1$, Eq. (8) implicitly gives F_c; then Y_{Lu}/ac_c is computed from Eq. (7), and hence the contraction coefficient can be estimated, since it only depends on a/Y_{Lu}. Finally, Eq. (9) gives the relative gate opening a/Y_u. Therefore, by varying F_u, the upper boundary of the hysteresis region can be plotted in the $(\mathsf{F}_u, a/Y_u)$ diagram, together with the lower boundary given by the endpoint of constraint (1) (see Fig. 3, later in the text).

The contraction coefficient used in the present work is that proposed by Defina and Susin (2003), which was determined by fitting a set of accurate experimental data

$$\begin{cases} c_c = 1 - r(\vartheta)\sin(\vartheta) \\ \dfrac{a}{Y_{Lu}} = 1 - r(\vartheta)\left[1 - \cos(\vartheta)\right] \\ r(\vartheta) = 0.153\vartheta^2 - 0.451\vartheta + 0.727 \end{cases} \tag{10}$$

with ϑ a dummy parameter in the range $0 \leq \vartheta < 2.5$. Importantly, in the following we assume that, when the flow is submerged, the contraction coefficient is moderately affected by the flow establishing downstream against the gate (see, e.g. Cassan & Belaud, 2012; Castro-Orgaz, Mateos, & Dey, 2013), and we still use Eq. (10) to estimate the contraction coefficient.

We now consider the more general case when a subcritical flow is present just downstream of and possibly against the gate, and study when the different flow configurations shown in Fig. 1 can establish and when a dual solution occurs.

2.1   The non-interacting flow domain

In the configurations Ua_1, Ua_2, and Ua_3, the fluid flows under the gate without interacting with the gate since the flow depth is smaller than the gate opening. Flow conditions characterizing the above configurations are referred to as smooth flow conditions.

Flow configurations Ua_1 or Ua_2 can establish only if the depth of the downstream flow is smaller than the gate opening

$$\frac{a}{Y_d} \geq 1 \tag{11}$$

Recalling that the continuity equation allows to write

$$Y_u \mathsf{F}_\mathsf{u}^{2/3} = Y_d \mathsf{F}_\mathsf{d}^{2/3}, \tag{12}$$

constraint (11) can be written as

$$\frac{a}{Y_u} \geq \left(\frac{\mathsf{F_u}}{\mathsf{F_d}}\right)^{2/3} \tag{13}$$

Within the region of the $(\mathsf{F_u}, a/Y_u)$ diagram identified by the above constraint, the Ua_1 configuration can establish only if the momentum of the undisturbed upstream flow is lower than that of the downstream subcritical flow. This condition can be expressed as

$$Y_u \geq Y_d^{conj} \tag{14}$$

Constraint (14), with Eq. (12), is rewritten as

$$\mathsf{F_u} \leq \mathsf{F_d}\left(\frac{2}{R_d}\right)^{3/2} \tag{15}$$

with

$$R_d = -1 + \sqrt{1 + 8\mathsf{F_d^2}} \tag{16}$$

If constraint (15) is violated, then flow configuration Ua_2 can establish. The threshold Froude number corresponding to the endpoint of the interval (15) is indicated as

$$\mathsf{F_{L1}} = \mathsf{F_d}\left(\frac{2}{R_d}\right)^{3/2} \tag{17}$$

In the case of non-interacting flow, the hydraulic jump locates upstream of the gate section if $\mathsf{F_u} < \mathsf{F_{L1}}$, and downstream if $\mathsf{F_u} > \mathsf{F_{L1}}$.

The flow configuration Ua_3 can establish when supercritical to subcritical transition occurs downstream of the gate (mathematically, when constraint (15) is violated) and the gate opening is in the interval $Y_u \leq a \leq Y_d$, i.e.:

$$1 \leq \frac{a}{Y_u} \leq \left(\frac{\mathsf{F_u}}{\mathsf{F_d}}\right)^{2/3} \tag{18}$$
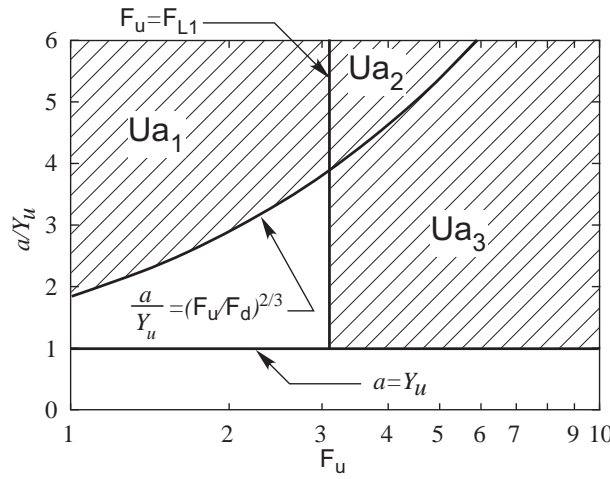
6

Figure 2   The non-interacting flow domain (the hatched area) in the (F_u, a/Y_u) diagram for $F_d=0.4$; the log-scale is used for F_u. The three configurations Ua_1, Ua_2, and Ua_3 are shown in Fig. 1.

It will be shown, later in the text, that when the gate opening is greater than the downstream flow depth, Ua_1 or Ua_2 are the only possible flow configurations. Accordingly, constraint (11) is not only a necessary condition for the occurrence of configurations Ua_1 or Ua_2, but it also a sufficient condition.

The regions of the (F_u, a/Y_u) diagram where configurations Ua_1, Ua_2, and Ua_3 can establish are shown in Fig. 2.

2.2   The free outflow domain

The free outflow configuration can establish only if (i) the jet of flow issuing from under the gate has a momentum that is large enough to push the downstream subcritical flow away from the gate, and (ii) the incoming supercritical flow has a momentum smaller than that of the subcritical flow just upstream of the gate.

The first condition, which identifies the upper boundary of the free outflow domain, can be written as (Lin, Yen, & Tsai, 2002)

$$ac_c \leq Y_d^{conj} \tag{19}$$

that is

$$\frac{a}{Y_u} \leq \frac{R_d}{2c_c} \frac{F_u^{2/3}}{F_d^{2/3}} \tag{20}$$

In order to estimate the upper boundary of the free outflow region, the contraction coefficient must be evaluated. On assuming free outflow condition, the energy balance equation between the *vena contracta* and the cross section just upstream of the gate is given by Eq. (5), which is here rearranged to read

$$\frac{Y_{Lu}}{ac_c} = 1 + \frac{F_u^2}{2} \frac{Y_u^3}{(ac_c)^3} \left[1 - \left(\frac{Y_{Lu}}{ac_c} \right)^{-2} \right] \tag{21}$$

7

At the endpoint of interval (20), i.e. when $a/Y_u = R_d \mathsf{F}_u^{2/3}/(2c_c \mathsf{F}_d^{2/3})$, Eq. (5) can be written as

$$\frac{Y_{Lu}}{ac_c} = 1 + \frac{4\mathsf{F}_d^2}{R_d^3}\left[1 - \left(\frac{Y_{Lu}}{ac_c}\right)^{-2}\right] \tag{22}$$

Among the three solutions of the above equation, the one of interest is

$$\frac{Y_{Lu}}{ac_c} = 2\left(\sqrt{1 + \frac{R_d^3}{\mathsf{F}_d^2}} - 1\right)^{-1} \tag{23}$$

For any given Froude number of the downstream flow, F_d, Eq. (23) gives Y_{Lu}/ac_c and hence the contraction coefficient can be estimated with, e.g. Eq. (10). With this, the upper boundary of the free outflow domain in the $(\mathsf{F}_u, a/Y_u)$ plane can be evaluated, being given by the endpoint of interval (20). The range of F_u within which constraint (20) actually ensures that free outflow configuration can establish is however limited by the second, necessary condition listed above, i.e. the momentum of the incoming flow must be smaller than that of the subcritical flow establishing just upstream of the gate. This condition is given by constraint (2), which, with Eqs. (23) and (12), can be written as

$$\frac{R_u}{\mathsf{F}_u^{2/3}} \leq \frac{2\mathsf{F}_d^{4/3}}{R_d^2}\left(1 + \sqrt{1 + \frac{R_d^3}{\mathsf{F}_d^2}}\right) \tag{24}$$

Let F_{L2} be the upstream Froude number corresponding to the endpoint of the above inequality. Since $R_u/\mathsf{F}_u^{2/3}$ increases monotonically with increasing F_u, constraint (24) gives the upper boundary of the free outflow region when F_u varies in the range $1 \leq \mathsf{F}_u \leq \mathsf{F}_{L2}$. When $\mathsf{F}_u \geq \mathsf{F}_{L2}$, the upper boundary of the free outflow domain corresponds to that given by Eq. (9) (i.e. the momentum of the incoming flow must be smaller than or equal to that of the subcritical flow establishing just upstream of the gate in order to ensure free outflow condition).

Beside F_{L1} and F_{L2}, a third, characteristic value of the upstream Froude number, which is here denoted with F_{L3}, is that given by the intersection of the upper boundary of the free outflow region with the line $a/Y_u=1$. Flow configuration Sb can occur only if $\mathsf{F}_u < \mathsf{F}_{L3}$. Using (20), we can write

$$\mathsf{F}_{L3} = \mathsf{F}_d\left(\frac{2c_c}{R_d}\right)^{2/3} \tag{25}$$

The lower boundary of the free outflow domain is, trivially, $a/Y_u=0$. For the case $\mathsf{F}_d=0.4$, the free outflow domain in the $(\mathsf{F}_u, a/Y_u)$ diagram is shown in Fig. 3.

2.3   The submerged outflow domain

The lower boundary of the submerged outflow domain corresponds to the upper boundary of the free outflow domain, which is given by Eq. (24) for $1 \leq \mathsf{F}_u \leq \mathsf{F}_{L2}$, and by Eq. (9) for $\mathsf{F}_u > \mathsf{F}_{L2}$.

As for the upper boundary, it is worth recalling that the submerged flow configuration can establish only if the momentum of the incoming flow is smaller than, or equal to, the momentum of the subcritical flow just upstream of the gate, as given by Eq. (2). With Eq. (3), the upper
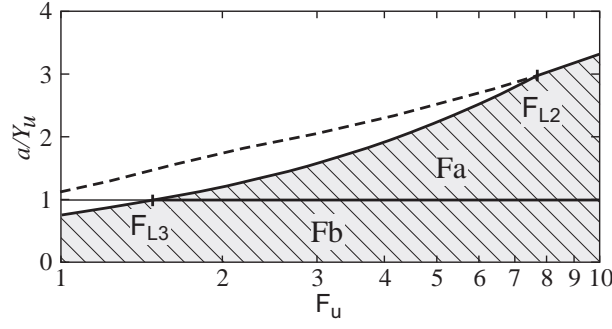
Figure 3   The free outflow domain (light grey hatched area) in the (F_u, a/Y_u) diagram for F_d=0.4. The dashed line is the upper boundary of the hysteresis region when downstream flow does not affect the flow through the gate (Eq. (9)); this boundary overlaps the present boundary for free outflow when $F_u > F_{L2}$.

boundary of the submerged flow domain, which is the endpoint of the interval (2), can be written as

$$\frac{Y_u}{ac_c}\frac{R_u}{2} = \frac{Y_{Lu}}{ac_c} \tag{26}$$

which is rearranged to read

$$\frac{a}{Y_u} = \frac{R_u}{2c_c}\left(\frac{Y_{Lu}}{ac_c}\right)^{-1} \tag{27}$$

In addition, Eq. (26), with Eq. (12), yields

$$\frac{R_u}{F_u^{2/3}} = \frac{2}{F_d^{2/3}}\frac{Y_{Lu}}{ac_c}\left(\frac{Y_d}{ac_c}\right)^{-1} \tag{28}$$

In order to assess the upper boundary of the submerged flow domain, we need to relate downstream flow conditions to flow conditions just upstream of the gate. This is achieved by using the energy-momentum method (Henderson 1966; see also Castro-Orgaz et al. 2013), which gives reliable results at least at the leading order of approximation.

Momentum balance equation between the downstream flow and the *vena contracta* cross section writes

$$\frac{Y_c^2}{2} + \frac{q^2}{gac_c} = Y_d^2\left(\frac{1}{2} + F_d^2\right) \tag{29}$$

which can be solved for Y_c to read

$$Y_c = Y_d\sqrt{1 + 2F_d^2\left(1 - \frac{Y_d}{ac_c}\right)} \tag{30}$$

The energy balance equation between the *vena contracta* and the cross section just upstream of

9

the gate gives

$$Y_c + \frac{q^2}{2g(ac_c)^2} = Y_{Lu} + \frac{q^2}{2gY_{Lu}^2} \tag{31}$$

Equation (31), with Eq. (30), yields

$$\frac{Y_{Lu}}{ac_c} = \frac{Y_d}{ac_c} \left\{ \sqrt{1 + \mathsf{F}_\mathsf{d}^2\left(1 - \frac{Y_d}{ac_c}\right)} + \frac{\mathsf{F}_\mathsf{d}^2}{2}\left(\frac{Y_d}{ac_c}\right)^2\left[1 - \left(\frac{Y_{Lu}}{ac_c}\right)^{-2}\right] \right\} \tag{32}$$

For any given Froude number of the downstream flow, F_d, the set of equations (27), (28), and (32) together with (12) and with an equation relating c_c to Y_{Lu}/a (e.g. Eq. (10)), can be solved to give Y_d/ac_c, Y_{Lu}/ac_c, c_c, F_u, and a/Y_u.

To solve the above set of equations, the following procedure can be adopted. Using Y_d/ac_c as a dummy variable, Y_{Lu}/ac_c is computed from Eq. (32). After estimating the contraction coefficient with Eq. (10), the upstream Froude number, F_u, is computed from Eq. (28). The relative gate opening, a/Y_u, is finally evaluated from Eq. (27). The interval within which Y_d/ac_c can vary is determined by observing that, with reference to Fig. 1, the flow depth Y_c can vary in the range

$$ac_c \leq Y_c \leq Y_d \tag{33}$$

Using Eq. (30), and after some algebra, the above interval for Y_c gives the range within which Y_d/ac_c is allowed to vary, reading

$$1 \leq \frac{Y_d}{ac_c} \leq \frac{2}{R_d} \tag{34}$$

The left inequality of constraint (34) implies that the depth of the downstream flow must be greater than the gate opening (indeed, under submerged flow conditions, $Y_d = ac_c$ entails $c_c = 1$, see Appendix A). The left endpoint thus corresponds to a particular condition in which the downstream flow depth is equal to both the gate opening and the subcritical flow depth just upstream the gate (i.e. $Y_d = a = Y_{Lu}$). The right inequality of constraint (34) implies that the downstream flow has a momentum that is greater than that of the undisturbed flow at the *vena contracta*. Accordingly, the right endpoint exactly corresponds to the upper boundary of the free outflow domain given by Eq. (24). This can easily be shown by solving Eq. (12) for Y_d and by substituting the result in the constraint (34).

The upper boundary of the submerged flow region, with F_u in the interval $\mathsf{F}_{\mathsf{L}1} \leq \mathsf{F}_\mathsf{u} \leq \mathsf{F}_{\mathsf{L}2}$, can be determined by varying Y_d/ac_c in the range given by Eq. (34). The assessment of the upper boundary for $1 \leq \mathsf{F}_\mathsf{u} \leq \mathsf{F}_{\mathsf{L}1}$ is rather intriguing, since the condition $Y_d/ac_c=1$, i.e. the left endpoint of constraint (34), actually gives the solution for all the upstream Froude numbers in the above interval. To make this point clear, the constraint (33) is rewritten as

$$\frac{ac_c}{Y_d} \leq \frac{Y_c}{Y_d} \leq 1 \tag{35}$$

Figure 4 shows how ac_c/Y_d and Y_c/Y_d vary with a/Y_u, when $\mathsf{F}_\mathsf{d}=0.4$ and $\mathsf{F}_\mathsf{u}=2.0$ (i.e. $1 \leq$
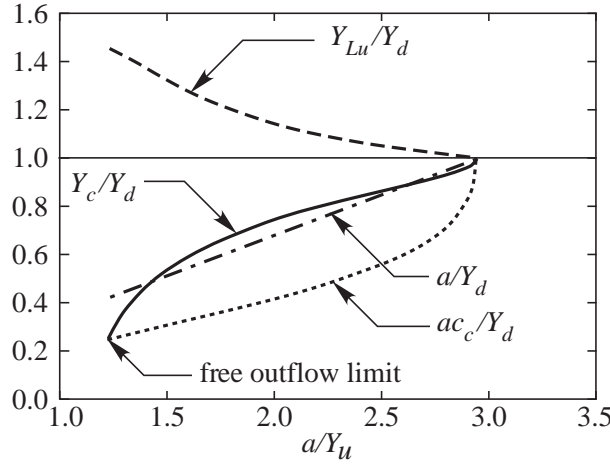
Figure 4 Y_{Lu}/Y_d, Y_c/Y_d, a/Y_d, and ac_c/Y_d as a function of a/Y_u for $\mathsf{F_d}$=0.4 and $\mathsf{F_u}$=2.0.

$\mathsf{F_u} \leq \mathsf{F_{L1}}$=3.1). The constraint (35) is satisfied when a/Y_u ranges from the free outflow limit (i.e. a/Y_u=1.23) to when $ac_c = Y_c = Y_d$ (i.e. a/Y_u=2.92). At the latter endpoint, we also have $Y_{Lu} = a = Y_d$, that is, here Eq. (A3) holds and leads to the same conclusions drawn above, that is, the upper boundary of the submerged flow domain corresponds to the lower boundary of the $\mathsf{Ua_1}$ smooth flow configuration. This conclusion is independent of $\mathsf{F_d}$ and $\mathsf{F_u}$ provided that $1 \leq \mathsf{F_u} \leq \mathsf{F_{L1}}$.

Therefore, ultimately, the upper boundary of the submerged flow domain is given by the constraint (13) when $1 \leq \mathsf{F_u} \leq \mathsf{F_{L1}}$, and by the solution to the set of equations (27), (28), (32), and (10), when $\mathsf{F_{L1}} \leq \mathsf{F_u} \leq \mathsf{F_{L2}}$. When $\mathsf{F_u} \geq \mathsf{F_{L2}}$, as stated above, the submerged flow configuration cannot establish because the flow issuing from under the gate has a momentum that is large enough to push away the downstream subcritical flow.

It is interesting to observe, in Fig. 4, that the flow depth Y_c is either greater or smaller than the gate opening, depending on the ratio a/Y_u. When $Y_c > a$ the $\mathsf{Sa_1}$ configuration establishes, otherwise, the $\mathsf{Sa_2}$ configuration occurs. Therefore, it is of interest to determine the boundary $Y_c = a$ between the two configurations. With Eq. (30), the condition $Y_c = a$ can be written as

$$\frac{Y_d}{ac_c}\sqrt{1 + 2\mathsf{F_d^2}\left(1 - \frac{Y_d}{ac_c}\right)} = \frac{1}{c_c} \tag{36}$$

For any given $\mathsf{F_d}$, the set of equations (32), (36), and (10), can be solved to give Y_d/ac_c, Y_{Lu}/ac_c, and c_c. This set of equations has two, out of nine, physically acceptable solutions for Y_d/ac_c, since both Y_d and Y_{Lu} must be real and positive, and the flow just upstream of the gate must be subcritical. However, given the strong nonlinearity of the equations of the set, explicit expressions for the two solutions are not available. It is worth noting that the two solutions only depend on $\mathsf{F_d}$, i.e. they are independent from $\mathsf{F_u}$.

In order to assess the two boundaries $Y_c = a$ in the ($\mathsf{F_u}$, a/Y_u) plane, we use the continuity Eq. (12) rewritten to read

$$\frac{Y_u}{a} = \frac{Y_d}{a}\frac{\mathsf{F_d^{2/3}}}{\mathsf{F_u^{2/3}}} \tag{37}$$

With the two solutions for Y_d/a, Eq. (37) describes the two boundary curves a/Y_u as a function of $\mathsf{F_u}$, separating the $\mathsf{Sa_1}$ from the $\mathsf{Sa_2}$ sub-domains. The interval within which $\mathsf{F_u}$ can vary extends
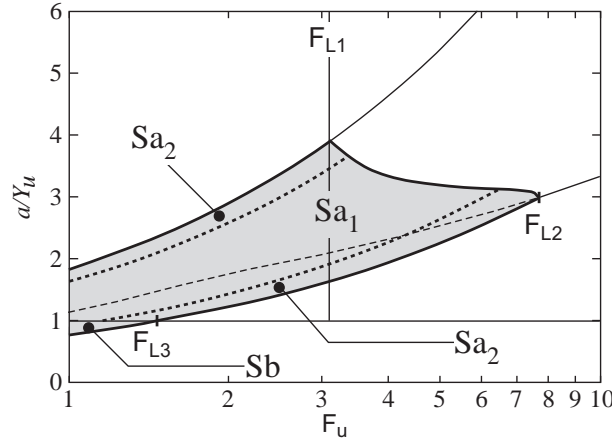
Figure 5   Submerged outflow domain (shaded area) in the (F_u, a/Y_u) diagram for F_d=0.4. The thick, dotted lines correspond to the condition $Y_c = a$ and separate the Sa$_1$ from the Sa$_2$ sub-domains.

from F_u=1 up to a threshold value that is determined by the constraint (2), which, with Eq. (12), can be rearranged to read

$$\frac{R_u}{F_u^{2/3}} \leq \frac{2}{F_d^{2/3}} \frac{Y_{Lu}}{Y_d} \tag{38}$$

The above inequality constraint, with the two solutions for Y_d/ac_c and Y_{Lu}/ac_c, hence, with the two solutions for Y_{Lu}/Y_d, allows to compute the two upper threshold values of F_u.

Figure 5 shows the submerged flow domain for the case F_d=0.4, together with the boundary curves separating the Sa$_1$ from the Sa$_2$ sub-domains. Sa$_2$ sub-domains, in the (F_u, a/Y_u) diagram, are shaped as two thin strips next to the upper and lower boundaries of the submerged flow domain. The width of these strips depends on the Froude number of the downstream flow. Specifically, their width increases with increasing F_d (see Fig. 6); the internal boundaries of these sub-domains (the two dotted curves of Fig. 6) move one toward the other until they overlap, leading to the disappearance of the Sa$_1$ configuration domain. This happens when F_d is greater than the threshold value F_{D1}=0.437.

To better illustrate this behaviour, we plot Y_c/a as it varies with a/Y_u for different values of the upstream and downstream Froude numbers (Fig. 7). The curves for $F_d < F_{D1}$ intersects the line Y_c/a=1 at two points, namely $(a/Y_u)_1$ and $(a/Y_u)_2$, with $(a/Y_u)_1 < (a/Y_u)_2$. Between these points, Y_c is greater than a and the Sa$_1$ configuration can establish; when $a/Y_u < (a/Y_u)_1$ or $a/Y_u > (a/Y_u)_2$, Y_c turns out to be smaller than a and the Sa$_2$ configuration can establish. The curves for $F_d > F_{D1}$ have no intersection with the line Y_c/a=1; they remain below this line so that Y_c is always smaller than the gate opening, i.e. Sa$_1$ configuration is not possible, and when the flow is submerged, only Sa$_2$ configuration can occur.

2.4   The hysteresis domains

In the previous sections, the domains for non-interacting flow, free outflow, and submerged outflow configurations have been determined and shortly discussed. By composing these domains, some of them are shown to overlap, thus indicating that two different states can establish for the same gate opening and flow conditions.

Figure 8 shows, for the case F_d=0.4, the results of this superposition. As expected, overlapping only occurs if $F_u \geq F_{L1}$, i.e. when smooth flow conditions for the incoming supercritical flow can
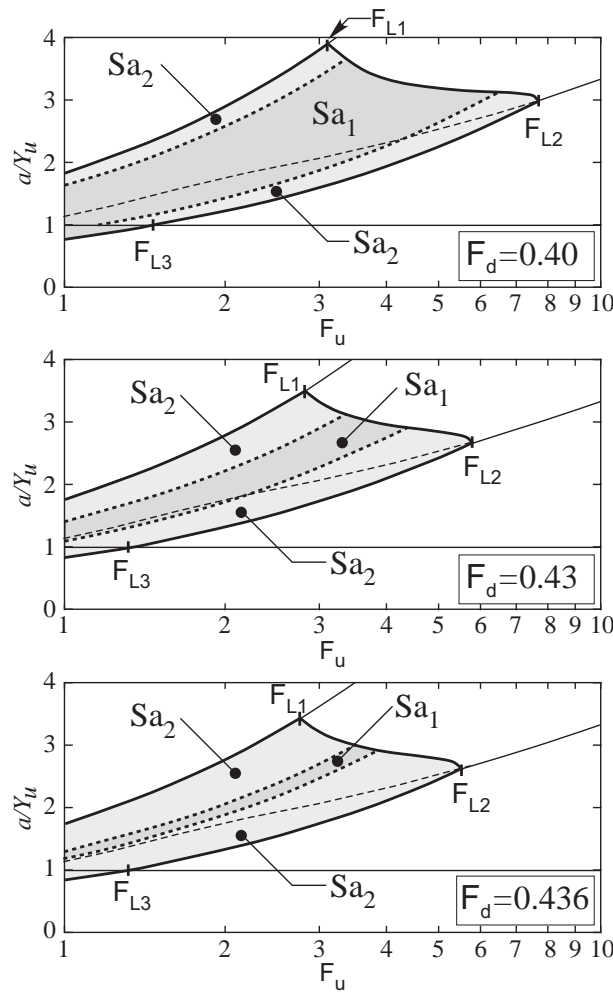
Figure 6   Submerged outflow domain in the (F_u, a/Y_u) diagram for three values of the downstream Froude number, F_d=0.4, 0.43, and 0.436. The thick, dotted lines correspond to the condition $Y_c = a$ and separate the Sa_1 sub-domain (dark grey) from the Sa_2 sub-domains (light grey).

establish. On the contrary, when $F_u < F_{L1}$, no double solution exists; this is not surprising since, to some extent, conditions in this range are equivalent to the case of subcritical incoming flow, for which hysteresis is not possible (Defina and Susin, 2003). Dual solution occurs in the hatched, dark grey region of Fig. 8 (resulting from the superposition of the hatched Ua_3 region of Fig. 2 and the dark grey region of Fig. 5). In this region, both smooth flow condition (Ua_3) and submerged flow condition (either Sa_1 or Sa_2) can establish. This region is referred to as submerged outflow hysteresis domain. Dual solution also occurs in cross-hatched, light grey region of Fig. 8 (resulting from the superposition of the hatched Ua_3 region of Fig. 2 and the hatched, light grey region of Fig. 3). In this region, both smooth flow condition (Ua_3) and free outflow condition (Fa) can establish. This region is referred to as free outflow hysteresis domain. It is worth noting that this region is a part of the hysteresis domain determined by Defina and Susin (2003).

In order to clarify what is meant by hysteretic behaviour, consider for example the case of F_d=0.4 and F_u=3.5 (i.e. $F_{L1} \leq F_u \leq F_{L2}$) and see the configurations that establish by raising and lowering the gate (Fig. 9). Let us start from smooth flow condition (Ua_2 configuration) with $a \gg Y_u$ (point I in Fig. 9), and gradually lower the gate. As long as the gate opening remains greater than the upstream flow depth, smooth flow conditions persist (Ua_2 configuration from point I to point II, and Ua_3 configuration from point II to point III). As soon as the edge of gate touches the free surface or just enters the flow, free outflow configuration (Fb) quickly establishes (point IV). Free
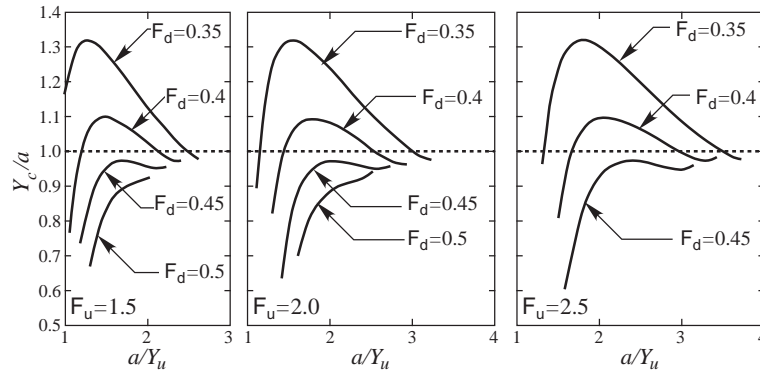
13

Figure 7 Y_c/a as a function of a/Y_u for different values of F_d (F_d=0.35, 0.4, 0.45, 0.5) and three values of the upstream Froude number, namely F_u=1.5, 2.0, and 2.5.
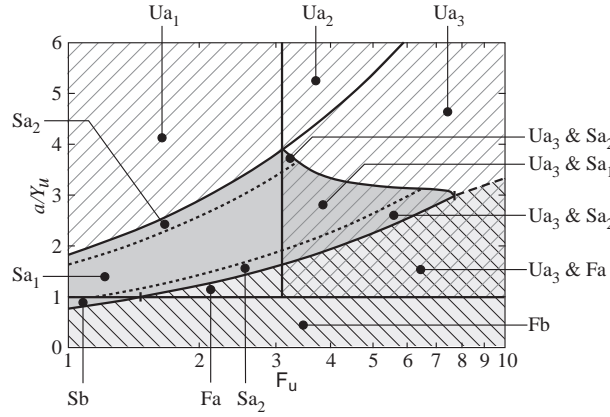

Figure 8 Domains of existence of different flow states for flow through a vertical sluice gate in the (F_u, a/Y_u) diagram for a downstream Froude number F_d=0.4. Symbols are the same as in Fig. 1, shading and hatching are the same as in Figs. 2, 3, and 5.
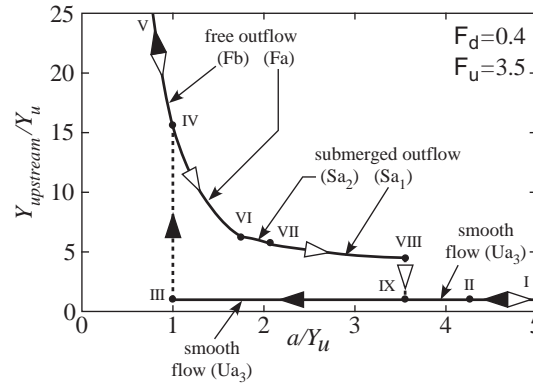

Figure 9 The hysteretic cycle for the case F_d=0.4 and F_u=3.5. $Y_{upstream}$ is the water depth just upstream of the gate, i.e. either Y_u (for smooth flow configuration) or Y_{Lu} (for free or submerged outflow). Point I, initial smooth flow configuration; point IX, restored smooth flow configuration. Black and white arrows denote the gate lowering and gate lifting stages, respectively.

outflow persists not only as the gate is lowered and/or raised along the branch from VI to V (Fb configuration), but also when the gate is raised along the branch from IV to VI (Fa configuration), i.e. until the relative gate opening $a/Y_u \approx 1.8$ is reached. Further opening of the gate produces submerged flow condition (Sa$_2$ configuration as long as $a/Y_u < 2.1$, i.e. from point VI to point VII, and Sa$_1$ configuration for larger gate opening, i.e. from point VII to point VIII). Smooth flow condition (i.e. Ua$_3$ configuration) is recovered only when the relative gate opening becomes greater
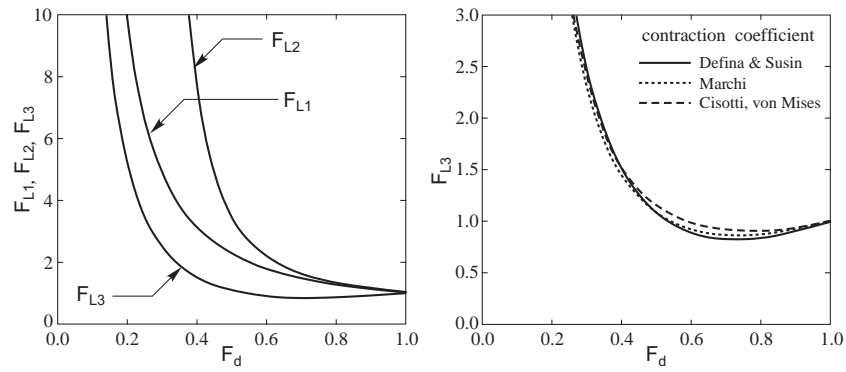
Figure 10   Left panel: upstream Froude number limits F_{L1}, F_{L2}, and F_{L3} as a function of F_d. Right panel: F_{L3} as a function of F_d computed with three different formulations for the contraction coefficient, i.e. those proposed by Defina and Susin (2003), by Marchi (1953) for gravity-affected flows, and by Cisotti (1908) and von Mises (1917) for gravity-free flows, as reported by Defina and Susin (2003).

than approximately 3.5 (point IX).

In this example, the a/Y_u interval within which two different flow configurations can establish is relatively large, since it extends from $a = Y_u$ to $a = 3.5Y_u$. More precisely, both Ua_3 and Fa configurations can establish when the relative gate opening is approximately in the range $1 \leq a/Y_u < 1.8$, and both Ua_3 and Sa_1 or Sa_2 configurations can establish when the relative gate opening is in the range $1.8 < a/Y_u < 3.5$.

With respect to the upstream Froude number, both the hysteresis domains are bounded below by $F_u = F_{L1}$; the free outflow hysteresis domain is unbounded above, whereas the submerged outflow hysteresis domain is bounded above by $F_u = F_{L2}$. It is therefore of interest to see how F_d affects the threshold values of the upstream Froude number. To this purpose, the left panel of Fig. 10 shows the threshold Froude numbers F_{L1}, F_{L2}, and F_{L3} as a function of the downstream Froude number, F_d. At small F_d, all the threshold Froude numbers quickly grow to extremely high values; this makes hysteresis unlikely to occur in practical cases if F_d is smaller than 0.3-0.4.

At relatively high values of F_d (i.e. F_d greater than 0.7-0.8), the curves for F_{L1} and F_{L2} nearly overlap so that the domain of submerged outflow hysteresis turns out to be extremely small; when $F_d=1$, we have $F_{L1}=F_{L2}=1$. At this extreme case, the double solution region with submerged outflow is reduced to a point and the hysteresis region turns out to coincide with that found by Defina and Susin (2003).

We also observe that the limit F_{L3} turns out to be smaller than one when F_d is greater than a threshold value of the downstream Froude number, i.e. $F_{D2} \approx 0.53$. This is more clearly shown in the right panel of Fig. 10, where F_{L3} is computed using three different formulations for the contraction coefficient. In this range (i.e. $F_d \geq F_{D2}$), the Sb configuration cannot establish.

Figure 11 shows the domains and sub-domains of all the possible flow configurations, and the two dual solution regions, when the downstream Froude number is $F_d=0.2$, 0.3, 0.5, and 0.6. At small F_d (e.g. $F_d=0.2$), hysteresis can occur only when the Froude number of the incoming flow is extremely large. Hereof, it is worth recalling that at high Froude number (roughly, $F_u > 4$-5), the flow is likely to entrain air (Defina, Susin, & Viero, 2008; Kramer and Hager, 2005; Takahashi & Ohtsu, 2017) and this process strongly affects the dynamics so that the present theory no longer applies.

The amplitude of the hysteresis region, which is defined as the difference, Δa, between the gate opening at the upper and lower boundary of the hysteresis region (Defina and Susin, 2003), is a function of both F_d and F_u. However, as a first, rough approximation, larger amplitudes occur at smaller values of F_d (see Fig. 11).

Interestingly, within the range $F_{L1} < F_u < F_{L2}$, that is, when submerged flow hysteresis can occur, the amplitude of the hysteresis region is greater than that when submerged flow cannot establish.
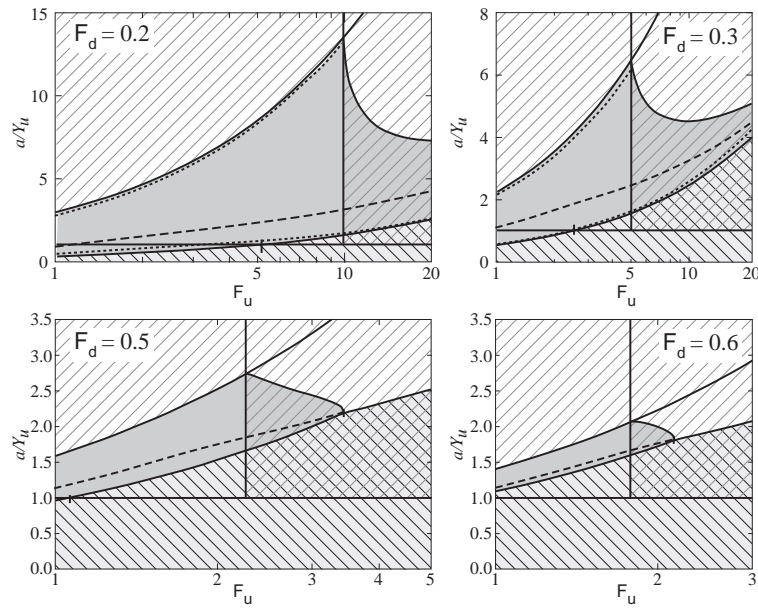
Figure 11 Domains of existence of different flow states for flow through a vertical sluice gate in the $F_u - a/Y_u$ diagram for four values of the downstream Froude number, i.e. F_d=0.2, 0.3, 0.5, 0.6. Symbols, shading and hatching are the same as in Fig. 8. The dashed line is the upper boundary of the hysteresis region in the absence of subcritical flow downstream of the gate.

For example, the relative amplitude is $\Delta a/Y_u$=0.9 for F_u=2.5, when only free outflow hysteresis can occur, whereas it is $\Delta a/Y_u$=1.6 for the same F_u, when F_d=0.5; the relative amplitude increases to $\Delta a/Y_u$=1.2 for F_u=3.5, when only free outflow hysteresis can occur, whereas it becomes as large as $\Delta a/Y_u$=2.5 for the same F_u, when F_d=0.4). As a rough guide, when the downstream Froude number is in the range 0.4-0.6, the relative amplitude of the hysteresis region, at F_u just greater than F_{L1}, is approximately twice the relative amplitude that is found, for the same F_u, when only free outflow hysteresis can occur.

3   Conclusions

A simple theoretical approach to predict conditions for the occurrence of hydraulic hysteresis for a supercritical flow approaching a sluice gate when subcritical flow can establish downstream, against the gate, has been proposed. It was shown that two different hysteresis regions exist in the (F_u, a/Y_u) plane; in one region both smooth flow condition (Ua$_3$ configuration) and submerged outflow condition (either Sa$_1$ or Sa$_2$ configuration) can establish, in the other region both smooth flow condition (Ua$_3$ configuration) and free outflow condition (Fa configuration) can establish. The boundaries of these regions, that depend on the Froude number of the downstream flow, have been determined.

It has been shown that, when submerged outflow establishes and flow conditions are within the range of submerged outflow hysteresis, the gate must be raised to openings higher, although not much higher, that the downstream subcritical flow in order to recover the smooth flow configuration (anyway, much greater than the depth of the incoming flow). This occurrence, as well as the other behaviours outlined and discussed in the present work, are of practical interest since sluice gates are widely used in laboratory experiments (e.g. Peruzzo, Viero, & Defina, 2016; Reichstetter & Chanson, 2013; Viero, Pradella, & Defina, 2017), as well as for flow control in open channels (Ansar & Chen, 2009; Triki, 2014, 2017), for example to control the upstream flow depth as an alternative to weir sills in the presence of large bedload. Thus, an in-depth knowledge of the hydraulic behaviour of this movable device is important in the effective design and operation of

flow control systems.

It has to be noted that the solutions obtained in this study, and shown in Figs. 2-11, can be moderately affected, from the quantitative point of view, by factors such as the use of correction coefficients for energy and momentum, and the actual value of the contraction coefficient, which depends on the type and the shape of the gate and on the Reynolds number as well (Belaud, Cassan, & Baume, 2012; Habibzadeh, Vatankhah, & Rajaratnam, 2011; Montes, 1997). However, these factors are not expected to affect the overall behaviour. Finally, we recall that the main goal of the present study was to demonstrate the existence of double solution domains in the flow through a sluice gate when the incoming flow is supercritical and subcritical flow is allowed to establish downstream against the gate and, especially, to suggest an effective theoretical approach to reconstruct all possible flow configurations.

Notation

a = gate opening (m)
c_c = contraction coefficient (–)
F = Froude number (–)
g = gravity acceleration (ms^{-2})
q = flow rate per unit width (m^{2}s^{-1})
Y = water depth (m)
Δa = amplitude of the hysteresis region (m)

Appendix A.

At the left endpoint of the interval (34), that is when $Y_d/ac_c = 1$, Eq. (32) reduces to

$$\frac{Y_{Lu}}{ac_c} = 1 + \frac{\mathsf{F}_d^2}{2}\left[1 - \left(\frac{Y_{Lu}}{ac_c}\right)^{-2}\right] \tag{A1}$$

which has three solutions

$$\frac{Y_{Lu}}{ac_c} = 1, \qquad \frac{Y_{Lu}}{ac_c} = \frac{\mathsf{F}_d^2}{4}\left(1 \pm \sqrt{1 + \frac{8}{\mathsf{F}_d^2}}\right) \tag{A2}$$

The two solutions on the right of (A2) are not acceptable, since one gives negative values for Y_{Lu}/ac_c, the other violates the constraint (2), which ensures that subcritical flow, with water depth Y_{Lu}, can establish just upstream of the gate. Therefore, at the left endpoint of the interval (34), with $Y_{Lu}/ac_c = 1$ (hence $c_c = 1$), and recalling (33), we have

$$Y_{Lu} = Y_d = ac_c = a = Y_c \tag{A3}$$

The above multiple equality makes sense if, and only if, $a = Y_d$, that is when the downstream subcritical flow almost touches the edge of the gate.

References

Abecasis, F. M. & Quintela, A. C. (1964). Hysteresis in steady free-surface flow. Water Power, 4, 147–151.

Akers, B. & Bokhove, O. (2008). Hydraulic flow through a channel contraction: Multiple steady states. Phys. Fluids, 20, 056601.

Ansar, M. & Chen, Z., (2009). Generalized flow rating equations at prototype gated spillways. J. Hydraul. Eng., ASCE, 135 (7), 602–608.

Austria, P. M. (1987). Catastrophe model for the forced hydraulic jump. J. Hydraul. Res., 25 (3), 269–280.

Baines, P. G. (1984). A unified description of two-layer flow over topography. J. Fluid Mech., 146, 127–167.

Baines, P. G. & Whitehead, J. A. (2003). On multiple states in single-layer flows. Phys. Fluids, 15 (2), 298–307.

Belaud, G., Cassan, L., & Baume, J. P. (2009). Calculation of contraction coefficient under sluice gates and application to discharge measurement. J. Hydraul. Eng., ASCE, 135 (12), 1086–1091.

Belaud, G., Cassan, L., & Baume, J. P. (2012). Contraction and correction coefficients for energy-momentum balance under sluice gates. In World Environmental And Water Resources Congress: crossing boundaries., E. D. Loucks (Ed.), Reston, VA: American Society of Civil Engineers, 2116–2127.

Cassan, L., & Belaud, G. (2012). Experimental and Numerical Investigation of Flow under Sluice Gates. J. Hydraul. Eng., ASCE, 138 (4), 367–373.

Castro-Orgaz, O., Mateos, L., & Dey, S. (2013). Revisiting the Energy-Momentum Method for Rating Vertical Sluice Gates under Submerged Flow Conditions. J. Irrigation and Drainage Eng.,ASCE, 139 (4), 325–335.

Cisotti, U. (1908). Vene fluenti. Rend. Circ. Mat. Palermo, 25, 145–179.

Defina, A. & Susin, F. M. (2003). Hysteretic behavior of the flow under a vertical sluice gate. Phys. Fluids, 15 (9), 2541–2548.

Defina, A. & Susin, F. M. (2006). Multiple states in open channel flow. In Vorticity and turbulence effects in fluid structures interactions - Advances in Fluid Mechanics, M.Brocchini and F.Trivellato (Ed.), Southampton: Wessex Insitute of Technology Press, UK, 105–130.

Defina, A., Susin, F. M. & Viero, D. P. (2008). Bed friction effects on the stability of a stationary hydraulic jump in a rectangular upward sloping channel. Phys. Fluids, 20, 036601.

Defina, A. & Viero, D. P. (2010). Open channel flow through a linear contraction. Phys. Fluids, 22, 036602.

Habibzadeh, A., Vatankhah, A. R., & Rajaratnam, N. (2011). Role of energy loss on discharge characteristics of sluice gates. J. Hydraul. Eng., ASCE, 137 (9), 1079–1084.

Henderson, F. M. (1966). Open channel flow, MacMillan Publishing Co., NewYork, 67–75.

Kramer, K. & Hager, W. H. (2005). Air transport in chute flows. Int. J. Multiph. Flow., 31, 1181–1197.

Lawrence, G. A. (1987). Steady flow over an obstacle. J. Hydraul. Eng., ASCE, 113 (8), 981–991.

Lin, C. H., Yen, J. F. & Tsai, C. T. (2002). Influence of Sluice Gate Contraction Coefficient on Distinguishing Condition. J. Irrig. Drain. Eng., ASCE, 128, 249–252.

Marchi, E. (1953). Sui fenomeni di efflusso piano da luci a battente. Ann. Matem. Pura e Appl. 35, 327–341.

Mehrotra, S. C. (1974). Hysteresis effect in one- and two-fluid systems. In D. Lindley & A. J. Sutherland (Eds.), V Australasian Conference on Hydraulics and Fluid Mechanics, University of Canterbury, Christchurch, New Zealand, 2, 452–461.

Montes, J. S. (1997). Irrotational flow and real fluid effects under planar sluice gates. J. Hydraul. Eng., ASCE, 123 (3), 219–232.

Muskatirovic, D. & Batinic, D. (1977). The influence of abrupt change of channel geometry on hydraulic regime characteristics. 17th IAHR Congress, Baden Baden, A, 397–404.

Peruzzo, P., Viero, D. P., & Defina, A. (2016). A semi-empirical model to predict the probability of capture of buoyant particles by a cylindrical collector through capillarity. Adv. Water Res., 97, 168–174.

Pratt, L. J. (1983). A note on nonlinear flow over obstacles. Geophys. Astrophys. Fluid Dynamics, 24, 63–68.

Sadeghfam, S., Khatibi, R., Hassanzadeh, Y., Daneshfaraz, R., & Ghorbani, M. A. (2017). Forced Hydraulic Jumps Described by Classic Hydraulic Equations Reproducing Cusp Catastrophe Features. Arab. J. Sci. Eng., 42, 4169–4179.

Reichstetter, M. & Chanson, H. (2013). Negative surges in open channels: physical and numerical modeling. J. Hydraul. Eng., ASCE, 139(3), 341–346.

Takahashi, M. & Ohtsu, I. (2017). Effects of inflows on air entrainment in hydraulic jumps below a gate. J. Hydraul. Res., 55(2), 259–268.

Triki, A. (2014). Resonance of free-surface waves provoked by floodgate maneuvers. J. Hydrol. Eng., ASCE, 19(6), 1124–1130.

Triki, A. (2017). Further investigation on the resonance of free-surface waves provoked by floodgate maneuvers: Negative surge waves. Ocean Eng., 133, 133–141.

Viero, D. P. & Defina, A. (2017). Extended theory of hydraulic hysteresis in open channel flow. J. Hydraul. Eng., ASCE, 143(9), 06017014.

Viero, D. P., Peruzzo, P., & Defina, A. (2017). Positive Surge Propagation in Sloping Channels. Water, 9(7), 518.

Viero, D. P., Pradella, I., & Defina, A. (2017). Free surface waves induced by vortex shedding in cylinder arrays. J. Hydraul. Res., 55(1), 16–26.

von Mises, R. (1917). Berechnüng von Ausfluss und Überfallzahlen. Z. Ver. Dtsch. Ing. 61, 447–452.